Analysis of the Performance Enhancement of MIMO Systems Employing Circular Polarization

Francesco Alessio Dicandia, *Student Member*, *IEEE*, Simone Genovesi, *Member, IEEE*, and Agostino Monorchio, *Fellow, IEEE*

***Abstract*— The advantages of adopting circular polarization in Multiple-Input-Multiple-Output (MIMO) systems are illustrated for both line-of-sight (LOS) and multipath propagation. More in detail, an analysis of the MIMO performance attainable by employing orthogonal circularly polarized (CP) radiators with respect to orthogonal linearly polarized (LP) ones, has been addressed. At first, an accurate analysis is presented aimed at the evaluation of the channel matrix by comprehensively including also the effects of the antenna in LOS condition. In particular, the channel matrix has been calculated as a function of the antenna parameters and orientation, demonstrating that CP radiators are capable of obtaining better average values of the matrix eigenvalues with respect to LP ones. The analysis is therefore completed by evaluating the characteristics of a CP MIMO system operating in indoor environment representing this latter a more challenging condition where multipath propagation occurs. In this latter case, some meaningful numerical experiments have been performed by using a reliable ray-tracing solver, followed by a measurements campaign conducted in a real environment for validation purposes. Measurements, which are in good agreement with simulations, confirm the benefits of adopting circular polarization in MIMO systems with respect to linear polarization.**

***Index Terms*—circular polarization (CP), Multiple input multiple output (MIMO), indoor propagation, polarization diversity, wireless local area network (WLAN) antenna.**

I. INTRODUCTION

The overwhelming growth of wireless communication systems as well as the increasing number of users have fostered the use of multiple antennas systems to cope with the imposed requirements and desired performance [1]. Indeed, a Multiple-Input-Multiple-Output (MIMO) system allows improving the spectral efficiency and guarantees, at the same time, a higher level of reliability of the overall radio communication link. Although MIMO employs multiple antennas, both at the receiver and the transmitter side, it does not require additional transmitted power or bandwidth with respect to a single-input-single-output (SISO) solution [2], [3]. In a MIMO system, the mitigation of multipath fading and minimization of antenna correlation coefficient are important tasks that have to be accomplished. The former goal has been pursued by polarization diversity [4]. For example, the use of single-band single-polarization scheme [5] or a dual-band dual-polarization one [6] have been applied within the ISM band. A cavity-backed linearly polarized wideband slot array has been adopted in [7] whereas an F- shaped linearly-polarized microstrip slot for quad-band operation is described in [8]. Dual polarized radiators for ultra wideband MIMO have been illustrated in [9] as well as in [10], where one radiator is designed for circular polarization and the other one operates in linear polarization. In [11], two co-located spiral dipoles, the former radiating a left-hand circular polarization (LHCP) and the latter a right-hand circular polarization (RHCP), provide good isolation even if other MIMO metrics have not been specified. On the other hand, a low coupling and correlation among MIMO elements is required to have good reliability and spectral efficiency and this is generally obtained with spatial diversity by placing at least half wavelength apart the antenna elements as well as by employing some isolation techniques [12]–[17].

It is interesting to notice that polarization diversity is often implemented by a dual-polarized antenna by exploiting linear polarizations [18]–[20]. However, compared to LP antennas, CP radiators exhibit several important advantages in terms of signal propagation. For instance, CP antennas are very effective in combating the multipath interferences and they are robust to polarization mismatch [21], [22]. For these reasons, the strength of the received signal is somewhat constant regardless of the CP antennas orientation. This characteristic is very useful for mobile communications where the receiving antenna continuously changes its position with respect to the transmitter.

Based on these considerations, CP antennas have been investigated as potential candidates for MIMO applications in order to improve the performances in terms of diversity gain (*DG*) or channel capacity (*C*). Indeed, although some CP MIMO antenna has been proposed [11], [23]–[25], the actual performances improvement provided by CP antennas in MIMO systems has not yet been demonstrated.

In our opinion, the use of orthogonal CP antennas in MIMO systems has not yet been carefully investigated and compared to MIMO systems adopting LP radiators. Therefore, an extensive study of the orthogonal CP MIMO system in both line of sight (LOS) condition and indoor multipath propagation is carried out in this paper. In particular, the advantages of adopting CP radiators in a MIMO system compared to LP ones will be illustrated at first by evaluating the channel matrix in LOS condition. It is important to highlight that the effect of the transmitting and receiving antennas is included in the channel matrix evaluation [26]. Moreover, the effect of the antenna pattern has been taken into account as well. A comparison in terms of eigenvalues (λ_i) of the channel matrix, the MIMO channel power gain and the channel capacity has been carried out in order to prove the advantages of exploiting the CP radiator rather than LP ones. Afterwards, the analysis of the received

power (P_r) for indoor propagation will be assessed by employing an in-house code based on ray-tracing (RT) technique [27] in order to take into account the multipath effect. In addition, the channel capacity has been also evaluated by using the Kroneker model and by performing measurements in a real indoor environment. To this purpose, some prototypes of MIMO antennas with two radiating elements have been designed and fabricated in microstrip technology.

The paper is organized as follows. The comparison between a MIMO system employing CP radiators and LP ones in LOS condition (accounting only for the direct ray) is presented in Section II by evaluating the eigenvalues, the MIMO channel power gain and the channel capacity. The following Section III analyses the received power within an indoor environment by a CP MIMO system with respect to a LP MIMO one. The comparison between the simulated and the measured channel capacity is addressed in Section IV. Conclusions are summarized in Section V.

II. LOS Propagation Case with CP and LP MIMO Antennas

In this Section, the benefits of using orthogonal CP radiators with respect to orthogonal LP ones is addressed for MIMO systems in LOS condition as a function of a three dimensional rotation. More in detail, the link between the transmitted and the received MIMO antenna is achieved by means of a single ray without taking into account the multipath phenomena. As it will be proved, the slower decrease of the depolarization factor provided by the CP radiators with respect the LP ones determines the better performance of CP antenna in a MIMO system. In fact, the ability of the CP radiators to provide a good link independently from the reciprocal position of equal-polarized elements, and the intrinsic isolation between radiators with different polarization, is at the basis of the difference between CP and LP. Moreover, the role of the Axial Ratio (AR) value in the depolarization factor trend will be also addressed.

In order to compare the MIMO performance, the LOS channel matrix (H_{LOS}) has been evaluated by using the scalar product (ξ) given by:

$$\xi = \underline{E}^{i} \cdot \underline{h}_{r} \qquad (1)$$

where $\underline{E}^{i}$ represents the incident electric field over the antenna element and $\underline{h}_{r}$ the received antenna effective height. By adopting this definition, the antennas are included in the channel model [26]. In Fig. 1*a*, a typical scenario where two MIMO antennas are in LOS condition is illustrated.

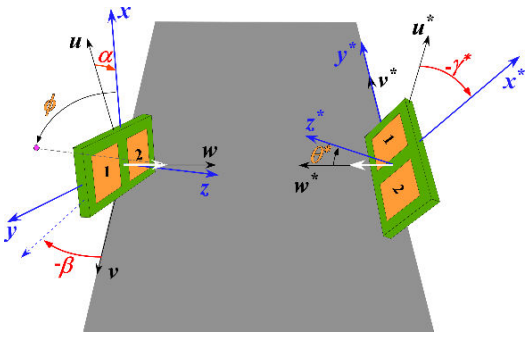

(a)

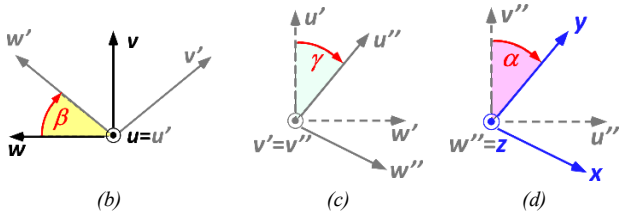

(b) (c) (d)

Fig. 1. *(a)* LOS environment with two MIMO antennas and their reference systems, rotation angle that the MIMO antenna can undergo: *(b)* angle β, *(c)* angle γ and *(d)* angle α.

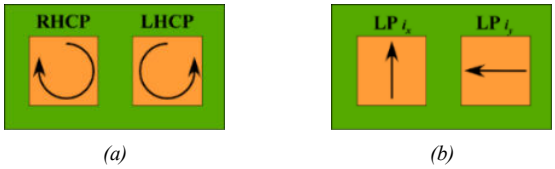

(a) (b)

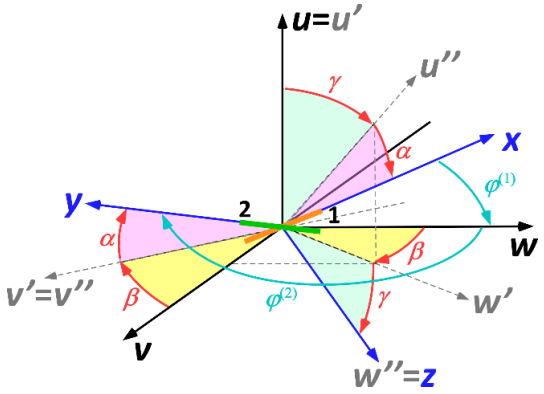

(c)

Fig. 2. *(a)* CP and *(b)* LP MIMO antennas with orthogonal polarization. *(c)* Reference systems of two collocated orthogonal LP radiators after α, β, γ rotation.

In order to define the rotation of each MIMO antenna, two sets of global axes are defined, namely (u, v, w) and (u^*, v^*, w^*). Next, an antenna local reference system is set with axis (x, y, z) and (x^*, y^*, z^*), respectively. These systems allow defining the correspondent three rotation angles (α, β, γ) and (α^*, β^*,γ^*) useful to transform the antenna local reference system (x, y, z) to the global fixed axes (u, v, w). For each rotation angle it is possible calculate a rotation matrix and the overall rotation matrix is obtained by multiplying together the individual matrices [28]. These three rotation angles are better explained in Fig. 1*b*-*c*-*d*. More in detail, β and β^* represent the rotation angle around u and u^* (Fig. 1*a*), the rotation angle around v' and v'* is defined as γ and γ^* (Fig. 1*b*) whereas α and α^* express the rotation angle around z and z^* (Fig. 1*c*).

Moreover, the angles (θ,ϕ) and (θ^*,ϕ^*) are defined between the antenna normal (z axis) and the line of sight direction (white arrow).

The considered CP and LP MIMO antennas can be of any technology (patch, slot), but they must exhibit orthogonal polarizations as shown in Fig. 2*a*-*b*, respectively. The comparison between the CP and LP radiators in MIMO system has been performed by keeping constant the dimension of the channel matrix (H), hence the number of the antenna elements. In particular, the performance enhancement of MIMO systems

employing CP radiators has been demonstrated only for two orthogonal radiators. Specifically, the channel matrix in LOS environment (H_{LOS}) has been evaluated with a rigorous mathematical approach whereas, in the multipath propagation scenario, the MIMO performance comparison have been carried out by both numerical simulations and measurements campaign. However, it seems reasonable to assert that an improvement can be also expected in case of more than two radiators by adopting orthogonally CP radiators instead of orthogonally LP ones. Nevertheless, if the elements are very close, such as in portable devices, the correlation between the radiators with the same polarization degrades the MIMO performance for both the orthogonally CP and LP MIMO system. For this reason, regarding LP radiators, a True Polarization Diversity (TPD) technique has been proposed to reduce the MIMO performance degradation when the radiators separation is very small (separation lower than 0.07λ) [29]. However, with the increasing of the radiators spacing, the benefit provided by TPD vanish, and the performance converge to that of the orthogonally LP MIMO system.

The effects of using CP radiators in MIMO systems with more than two radiators and with a very small elements separation needs further investigation. Additional analysis is also required to reduce the coupling between the radiators with the same polarization, and therefore reduce the MIMO performance degradation due to the high correlation.

A. LP Radiators

In order to evaluate the LP MIMO performance as a function of a three dimensional rotation angle of the MIMO antennas, three main rotation angles have been defined (Fig. 1), namely (α, β, γ) for the transmitter (T_x) and ($\alpha^*, \beta^*, \gamma^*$) for the receiver ($R_x$). In order to take into account the effect of the radiation pattern, the LP radiators effective height is set equal to that of a half wave dipole:

$$\underline{hLP}_k(\varphi_k) = \frac{\cos\left(\frac{\pi}{2}\cos(\varphi_k)\right)}{\sin(\varphi_k)} \quad k = 1,2 \tag{2}$$

where φ_k represents the angle between the dipole axis and the considered direction of radiation (w axis). By summarizing, the rotation angles (α, β, γ) that the MIMO antenna can undergo and the φ_k angles useful to evaluate the radiators effective height can be better understood through the Fig. 2*c* where two orthogonal dipoles located along x and y axes are illustrated.

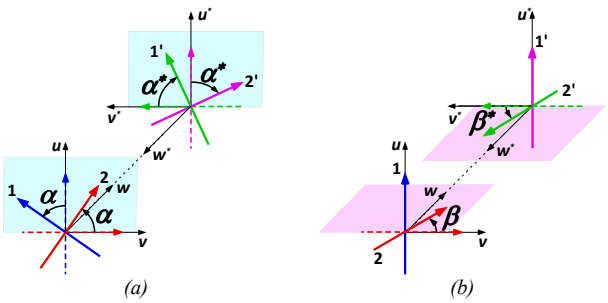

(a) *(b)*

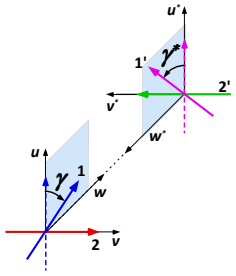

(c)

Fig. 3. MIMO antenna rotation angles; *(a)* α angle, *(b)* β angle *(c)* γ angle.

At the beginning, the channel matrix in LOS for the LP MIMO antenna has been evaluated by considering only one rotation angle. Assuming that the T_x-R_x MIMO antenna separation is sufficiently large, the two radiators of each MIMO antenna are considered co-located. For each rotation, the correspondent channel matrix is equal to:

$$H_{LOS_{(\alpha)}}^{(LP)} = \begin{bmatrix} \cos(\alpha+\alpha^*) & \sin(\alpha+\alpha^*) \\ \sin(\alpha+\alpha^*) & -\cos(\alpha+\alpha^*) \end{bmatrix}, \tag{3}$$

$$H_{LOS_{(\beta)}}^{(LP)} = \begin{bmatrix} 1 & 0 \\ 0 & -\underline{hLP}_2\left(\frac{\pi}{2}-\beta\right)\underline{hLP}_{2'}\left(\frac{\pi}{2}-\beta^*\right)\cos(\beta-\beta^*) \end{bmatrix}, \tag{4}$$

$$H_{LOS_{(\gamma)}}^{(LP)} = \begin{bmatrix} \underline{hLP}_1\left(\frac{\pi}{2}-\gamma\right)\underline{hLP}_{1'}\left(\frac{\pi}{2}-\gamma^*\right)\cos(\gamma+\gamma^*) & 0 \\ 0 & -1 \end{bmatrix} \tag{5}$$

where $hLP_k(\cdot)$ and $hLP_{k'}(\cdot)$ ($k = 1, 2$) represent the effective height calculated by considering the angle between the dipole axis and the LOS direction for the transmitter and the receiver MIMO antenna respectively. By observing (3), it can be noticed that the LP MIMO system does not undergo a decrease of the MIMO performance in case of α and α^* rotation around w and w^* axes, since $H H^*$ is equal to identity matrix (I). On the other hand, the other rotation angles do not determine the same results and then the performance will be obviously different.

By combining the channel matrixes obtained by only one rotation angle (3) - (5) and by using the overall rotation matrix [28], the entry of the total channel matrix for an arbitrary three-dimensional rotation can be evaluated for the LOS case. In particular, by assuming that the receiving MIMO antenna does not present any rotation ($\alpha^* = \beta^* = \gamma^* = 0°$), the entry of the total LOS channel matrix (H_{LOS}) is given by:

$$h_{11'_{LOS}}^{(LP)} = \underline{hLP}_1(\varphi_1)\cos(\gamma)\cos(\alpha) \tag{6}$$

$$h_{12'_{LOS}}^{(LP)} = \underline{hLP}_1(\varphi_1)\left[\sin(\beta)\sin(\gamma)\cos(\alpha)+\cos(\beta)\sin(\alpha)\right] \tag{7}$$

$$h_{21'_{LOS}}^{(LP)} = \underline{hLP}_2(\varphi_2)\cos(\gamma)\sin(\alpha) \tag{8}$$

$$h_{22'_{LOS}}^{(LP)} = \underline{hLP}_2(\varphi_2)\left[\sin(\beta)\sin(\gamma)\sin(\alpha)-\cos(\beta)\cos(\alpha)\right] \tag{9}$$

From equations (6)-(9) it can be inferred that the channel matrix of the LP MIMO system strongly depends on the antennas reciprocal orientation as confirmed by the significant variation of the channel gain $h_{ij'_{LOS}}^{(LP)}$.

B. CP Radiators

By employing CP radiators in the MIMO antenna system, the entry of the channel matrix H_{LOS} has been characterized by using the AR of the radiators as well as their radiation patterns. In particular, to obtain a CP field, two orthogonal LP radiators with a phase difference of 90° has been taken into account. For a CP radiator the effective height is set equal to:

$$\underline{hCP}_k(\theta,\phi,\varphi_k)=\frac{1}{\sqrt{1+AR^2(\theta,\phi)}}\underline{hLP}_k(\varphi_k)\left(\hat{i}_\theta+jAR(\theta,\phi)\hat{i}_\phi\right)\quad k=1,2 \tag{10}$$

where $AR(\theta,\phi)$ represents the axial-ratio of the transmitter. For the receiver elements, the AR is identified with $AR(\theta^*,\phi^*)$. The angles (θ,ϕ) and (θ^*,ϕ^*) depend from the antenna rotation angles α,β,γ and $\alpha^*,\beta^*,\gamma^*$ and represent the direction of the departing and incoming wave, respectively. Moreover, it is possible to notice that the transmitted power is the same as in the LP case, in order to have a fair comparison. By using (1) and assuming that the receiving MIMO antenna does not present any rotation ($\alpha^*=\beta^*=\gamma^*=0°$), the elements of the total channel matrix in case of CP radiators, are equal to:

$$h_{11'_{LOS}}^{(CP)}=\underline{hLP}_1(\varphi_1)\left(\frac{1+AR(\theta,\phi)AR(0,\phi^*)}{\sqrt{1+AR^2(\theta,\phi)}\sqrt{1+AR^2(0,\phi^*)}}\right) \tag{11}$$

$$h_{12'_{LOS}}^{(CP)}=\underline{hLP}_1(\varphi_1)\left(\frac{1-AR(\theta,\phi)AR(0,\phi^*)}{\sqrt{1+AR^2(\theta,\phi)}\sqrt{1+AR^2(0,\phi^*)}}\right) \tag{12}$$

$$h_{21'_{LOS}}^{(CP)}=\underline{hLP}_2(\varphi_2)\left(\frac{1-AR(\theta,\phi)AR(0,\phi^*)}{\sqrt{1+AR^2(\theta,\phi)}\sqrt{1+AR^2(0,\phi^*)}}\right) \tag{13}$$

$$h_{22'_{LOS}}^{(CP)}=\underline{hLP}_2(\varphi_2)\left(\frac{1+AR(\theta,\phi)AR(0,\phi^*)}{\sqrt{1+AR^2(\theta,\phi)}\sqrt{1+AR^2(0,\phi^*)}}\right) \tag{14}$$

C. LP and CP Radiators in MIMO Antenna System

By considering the equations (6)-(9) for LP radiators and the equations (11)-(14) for the CP ones, it can be proved that, by neglecting the effect of the radiation pattern, the entries of the channel matrix for a CP MIMO system depend only on the AR and not from the antennas reciprocal orientation. On the contrary, the performance of the LP MIMO system relies on the antennas positioning since the entries of the channel matrix depend on the orientation of the transmitter and receiver MIMO antenna. Moreover, by employing CP antennas, the level of the received power by each radiators is the same, which is proportional to $\left|h_{ii'_{LOS}}^{(CP)}\right|^2+\left|h_{ij'_{LOS}}^{(CP)}\right|^2$. On the contrary, the MIMO antenna orientation can generate an unbalance of the received power between the LP elements since $h_{11'_{LOS}}^{(LP)}$ is different from $h_{22'_{LOS}}^{(LP)}$. This unbalance may negatively affect the diversity gain [30], [31] and the channel capacity [32]. For this reason, the use of CP radiators in MIMO systems allows achieving a higher DG, thus a better reliability, and a better robustness with respect to the antenna orientation than the ones offered by LP antennas.

In order to compare the performances between MIMO systems employing CP or LP radiators, an AR model has been introduced as a function of the (θ,ϕ) angles. In particular, the considered AR model is a function of θ angle. This model considers an $AR_{dB}=\theta^4/K$ where θ is within (-90°;90°), $K=A^4/3$. Moreover, A expresses the angle (in degrees) within $AR_{dB}\leq 3$dB. For example, the AR model illustrated in Fig. 4*a* is obtained by setting $A=50$ degrees where the white line shows the curve for $AR=3$ dB. Moreover, in Fig. 4*b* is illustrated the same AR model expressed in (β,γ) angles. In Fig. 5, the AR model as a function of the A parameter is reported with respect to theta angle.

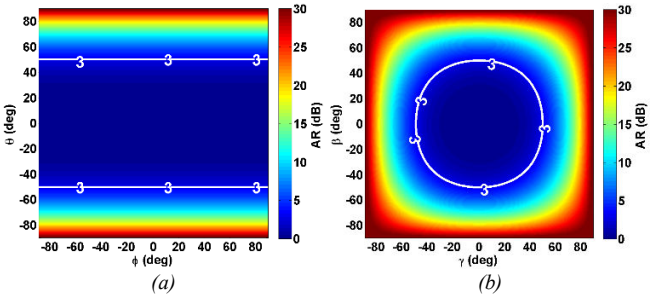

Fig. 4. AR model of the radiators for CP MIMO antenna *(a)* expressed in (θ,ϕ) angles and *(b)* (β,γ) angles.

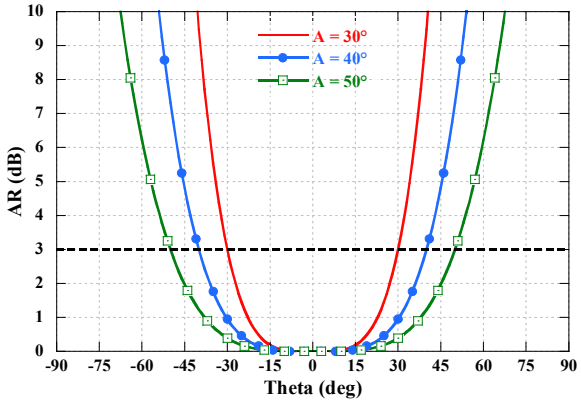

Fig. 5. AR model of the radiators for CP MIMO antenna for different value of A parameter as a function of the theta angle.

In order to compare the MIMO performance of the LP and CP radiators, the SVD (singular values decomposition) of the related channel matrix H_{LOS} has been used for calculating the eigenvalues (λ_i) of the matrix $H_{LOS}H^*_{LOS}$. Indeed, given the MIMO channel matrix, the MIMO system can offer K parallel SISO sub-channels with different gain where it is possible to send different streams of data [33], [34]. More in detail, $K=\mathrm{rank}(HH^*)\leq\min(n_t,n_r)$ represents the degree of freedom of the MIMO system whereas the eigenvalues (λ_i) represent the power gain of each *K-th* sub-channel. At this point, two scenarios are possible: absence of knowledge of the channel state information (CSI) at the transmitter, and knowledge of the CSI at the transmitter. In the former case, because of the absence of the CSI, the total transmitter power will be equally split to each *K- th* sub-channel. In the latter, with the knowledge of the CSI at the transmitter, it is possible to obtain an optimum power allocation for each *K-th* sub-channel (water filling technique) according to the related eigenvalues (λ_i) in order to optimize the spectral efficiency.

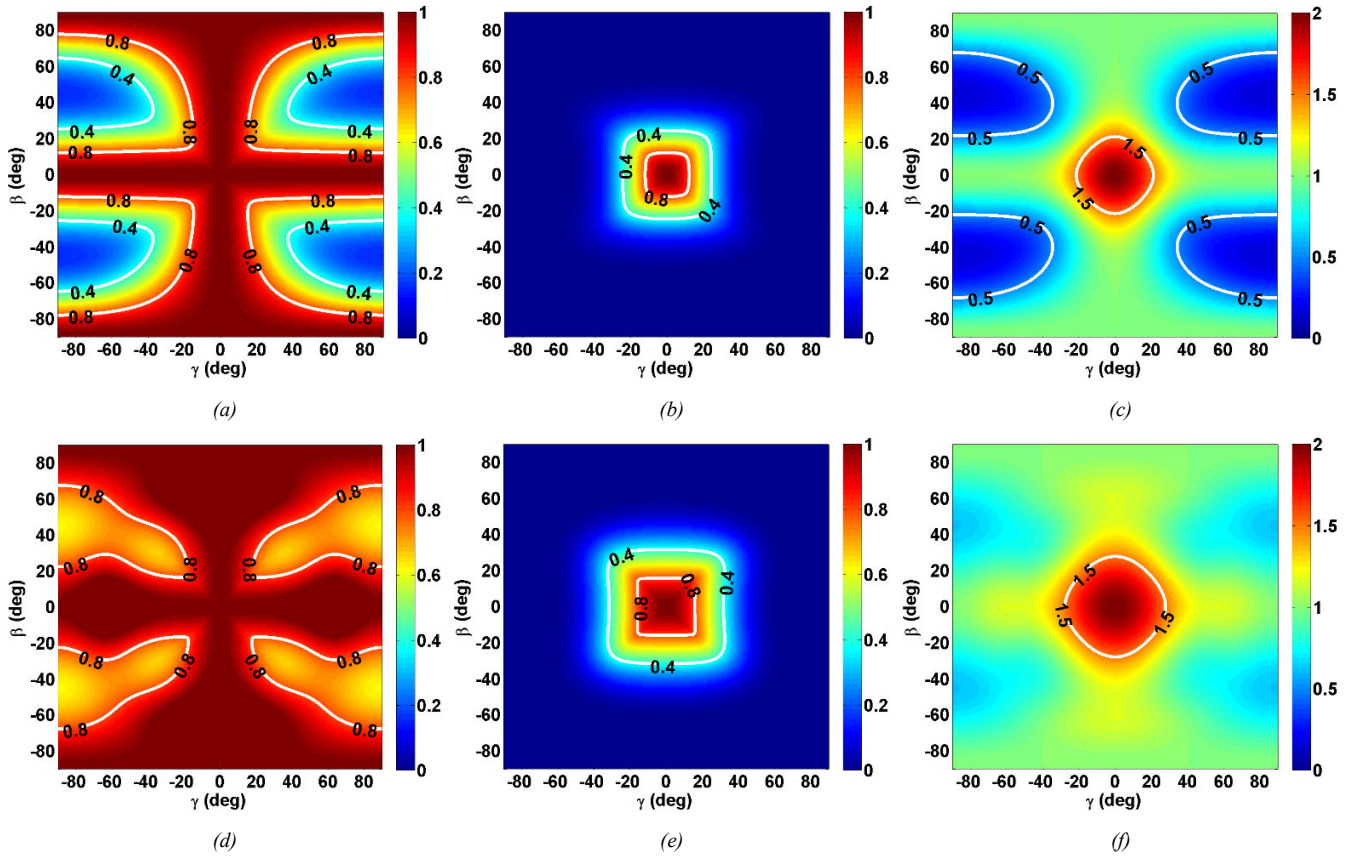

Fig. 6. *(a)* Eigenvalue λ_1 , *(b)* eigenvalue λ_2 and *(c)* MIMO channel power gain of the LP MIMO system; *(d)* eigenvalue λ_1 , *(e)* eigenvalue λ_2 and *(f)* MIMO channel power gain of the CP MIMO system with A=50°.

However, even if the water filling scheme provides the highest channel capacity, the difference with respect to the uniform power allocation (no CSI at the transmitter) is very small when the radiators of the MIMO antennas are sufficiently uncorrelated [34]. However, the CSI is not usually available at the transmitter [33], [35] and the knowledge of the CSI requires the transmission and the reception of pilot symbols through a reverse channel that is time consuming. This is even more critical when the channel changes quickly with a small coherence time [36], such as in the case of a mobile terminal. Therefore, the overhead for the reverse can be prohibitive [33]. Moreover, the knowledge of the CSI does not modify the eigenvalues (λ_i) but allows obtaining an optimal power allocation to enhance the spectral efficiency, as mentioned above.

In Fig. 6 the eigenvalues λ_1 and λ_2 and the MIMO channel power gain, defined as the sum of the square of eigenvalues, are reported as a function of the rotation (β, γ) of one MIMO antenna. The evaluation for the CP case has been obtained by using the previously introduced AR model with A = 50 degrees (Fig. 4). By comparing the obtained eigenvalues (Fig. 6 *a-b-d-e*) it can be concluded that the CP and LP radiators enable to achieve the same maximum performance when the MIMO antennas are perfectly aligned. However, when the MIMO antennas are not perfectly aligned, the CP radiators allow obtaining greater eigenvalues (λ_1 and λ_2) than the LP ones. This aspect can also observed by showing the MIMO channel power gain as a function of the MIMO antenna rotation (Fig. 6 *c-f*). Indeed, it is apparent that the CP radiators cover a greater area than the LP case for a fixed value of the channel power gain. It is therefore proved that the use of CP MIMO antennas provides a more robust MIMO system with respect to the antenna orientations than the one employing LP radiators.

In addition, the channel capacity (C) was evaluated as a function of the MIMO antenna orientation by using the channel matrix previously obtained (Fig. 7). In Fig. 7 the channel capacity in LOS condition and with no CSI at the transmitter is reported as a function of the rotation of one MIMO antenna for a fixed value of the signal-to-noise ratio (SNR) equal to 20 dB. More in detail, as previously reported, the maximum channel capacity is obtained when the MIMO antennas are aligned and there is no difference of channel capacity between the LP and CP radiators usage, due to the presence of two independent sub-channels with the same channel gain ($\lambda_1 = \lambda_2 = 1$). However, if the MIMO antennas are not perfectly aligned, which is a very likely situation for wireless communications systems, the channel capacity is greater for the CP case with respect to the LP ones. This aspect is better highlighted by showing the difference of the channel capacity between the CP and LP radiators, as it is presented in Fig. 7*c*. Indeed, it is apparent that, by employing CP antennas with A = 50°, the MIMO system is able to generate up to 1.5 b/s/Hz higher channel capacity than LP MIMO antennas

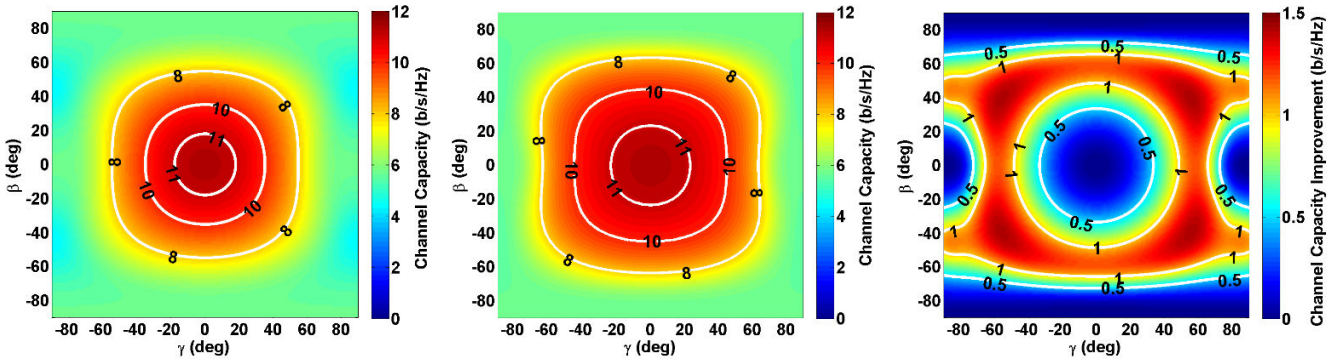

(a) *(b)* *(c)*

Fig. 7. Channel capacity (C) as a function of the MIMO antenna rotation angles when the SNR = 20 dB; *(a)* LP radiators, *(b)* CP radiators with A=50° and *(c)* channel capacity difference between the CP and LP MIMO antenna radiators.

(when the MIMO antennas are not aligned), as a result of the greater eigenvalues as previously shown in Fig. 6. Obviously, the maximum of the channel capacity improvement enhance more and more with the increasing of the angle where the AR has a value lower than 3 dB (A parameter) for the CP MIMO radiators.

This improvement of the MIMO performance as a function of the MIMO antennas orientation is due to a slower decrease of the depolarization factor provided by the CP radiators with respect to LP ones.

The impact of the polarization on the channel capacity has been also evaluated from a statistical point of view. More in detail, the cumulative distribution function (C.d.F) of the channel capacity has been taken into account with respect to the MIMO antenna orientation, for both LP and CP radiators (Fig. 8.). In particular, for the CP case, different conditions are taken into account, among which the ideal condition ($AR = 1$) and the worst one ($AR = \infty$). By looking at the Fig. 8, it is evident that an ideal CP radiator ($AR = 1$) generates the best performance in terms of C.d.F.

Indeed, the reduction of the capacity as a function of the MIMO antenna rotation is only due to the decreasing of the radiation pattern since, in this case, the depolarization factor is always equal to 1 for each MIMO antenna orientation. On the other hand, if the CP radiators generate a very high AR in all directions, the MIMO system can generate only one degree of freedom, hence the maximum achievable channel capacity is the half. In this case, the two CP radiators behave as two co-polar LP radiators.

In Table I, the mean value of the channel capacity and the probability that the $C > 8$ b/s/Hz, are reported. It can be observed that the exploitation of circular polarization in a MIMO system outperforms the linear one in a statistical point of view. More in detail, the better performance of CP radiators with respect to LP ones are highlighted by a higher mean value and a better statistical behaviour in terms of the C.d.F. of the channel capacity obtained in the case of ideal CP radiators ($AR = 1$). Obviously, the CP performance undergoes a degradation by decreasing the A parameter that expresses in degrees the angle at which $AR_{dB} = 3$dB.

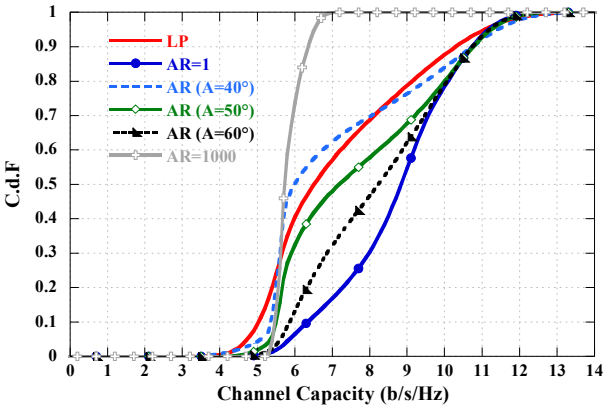

Fig. 8. Mean C.d.F of the channel capacity as a function of the MIMO antenna rotation by considering CP and LP radiators.

Moreover, the maximum value and the mean value (η) of the channel capacity improvement as a function of the A parameter for the CP radiators are shown in Table II. From the same Table II, the better robustness of the CP radiates with respect the LP one in MIMO systems are highlighted. Indeed, with an ideal CP radiators ($AR = 1$), the channel capacity improvement presents a max value of 4.37 b/s/Hz and a mean of 1.55 b/s/Hz.

By summarizing, through the Fig. 8, Table I and the Table II, it is evident that the same LP MIMO performance can be obtained by using CP radiators with $A = 40$ degrees. Indeed, by employing CP MIMO radiators with $A = 40°$, the MIMO system provides a slightly lower mean channel capacity than LP MIMO antenna, as shown in Table I. However, the CP radiators provide a better statistic behaviour confirmed by the same probability to have a $C > 8$b/s/Hz (Table I), a zero mean value of the channel capacity improvement and a maximum value of the channel capacity improvement of 0.96 b/s/Hz (Table II).

Based on this consideration, for all values of A greater than 40 degrees, the CP radiators enable to achieve better average performance than LP ones.

TABLE I
CHANNEL CAPACITY COMPARISON BETWEEN LP AND CP RADIATORS IN LOS

Radiators	Mean of Channel capacity (b/s/Hz)	$P_r(C > 8$ b/s/Hz)
LP	6.4	0.31
CP (*AR*=1)	8.9	0.7
CP (*AR* =∞)	5.7	0
CP (*A* =40°)	6	0.3
CP (*A*=50°)	7.2	0.43
CP (*A*=60°)	8.2	0.53

TABLE II
MAXIMUM AND MEAN OF THE CHANNEL CAPACITY IMPROVEMENT

CP Radiators	max{*C* Improvement} (b/s/Hz)	η (b/s/Hz)
CP (*AR*=1)	4.37	1.55
CP (*AR* =∞)	0.96	-1.3
CP (*A* =40°)	0.96	0
CP (*A*=50°)	1.23	0.58
CP (*A*=60°)	2.49	1.1

III. EFFECTS OF MULTIPATH PROPAGATION IN CP MIMO

To extend the previous results obtained in LOS and absence of multipath, the performance of the MIMO system has been tested also taking into account the multipath propagation. In particular, the P_r has been evaluated for some MIMO antennas in an indoor scenario by using an in-house reliable numerical solver based on ray-tracing technique [27]. To this purpose, orthogonal CP and LP MIMO antennas have been designed and realized in microstrip technology. It is important to underline again that the aim of this study is not to propose a particular MIMO antenna design, but to highlight the advantages of using CP radiators. Therefore, the two presented configurations (one CP and the other one LP) have the same footprint and exhibit similar patterns and S_{11} bandwidth to propose a fair comparison and to show how the better results only depends on the employed polarization.

A. MIMO Antennas Configuration

Each one of the two considered MIMO antenna systems comprises two microstrip patch antennas designed to operate within the WLAN band (2.4 – 2.5 GHz). The designed CP and LP MIMO antennas are illustrated in Fig. 9. In Fig. 9*a* two square patches with truncated corners and a U-shaped slot cuts [37] are shown and they both radiate a circular polarized electromagnetic field. The left one (Element # 1) exhibits a right-handed circularly-polarization (RHCP) whereas the adjacent element (Element # 2) is left-handed circularly-polarized (LHCP). The orthogonal LP MIMO antenna comprises two square patches printed on a grounded dielectric slab of the same dimension (Fig. 9*b*). Both systems have a compact footprint with an edge-to-edge antenna separation equal to 10 mm (nearly 0.08 λ_0 at 2.45 MHz), whereas the overall area is 72×36 mm^2. Both the designed MIMO antennas are printed on a FR4 substrate layer with thickness of 5 mm and are aligned along the H-plane (*v-axis*) in order to minimize the coupling. The simultaneous presence of both RHCP and LHCP and two orthogonal LP antenna elements, offers the possibility to exploiting the polarization diversity to decrease the correlation.

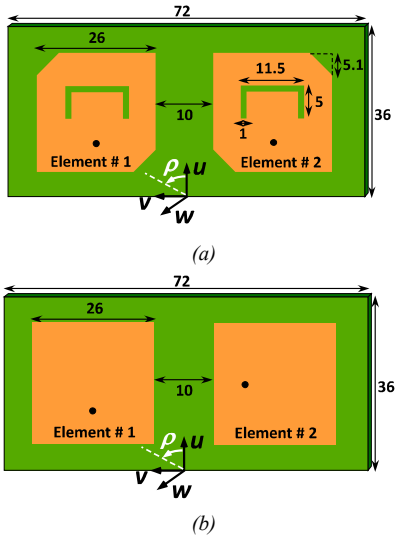

Fig. 9. Geometry of the two different MIMO antenna systems: *(a)* CP radiators and *(b)* LP radiators.

The patch antenna are aligned along their H-plane and, in order to obtain the lowest mutual coupling (S_{12}) between the antenna elements, four different orientations of Element #2 in the *u* - *v* plane (ρ angle) have been investigated for CP antenna configuration. From Fig. 10, it can be observed that the orientation of the *Element #2* minimizing the mutual coupling is $\rho = 0°$ (Fig. 9*a*).

The simulated *AR* in the upper hemisphere at 2.45 GHz is reported in Fig. 11 for Element #1 of CP MIMO configuration. This *AR* is very similar to the model proposed in Fig. 4*a* where the *AR* model totally depends on θ angles. All the antennas have been fabricated (Fig. 12) and experimentally characterized.

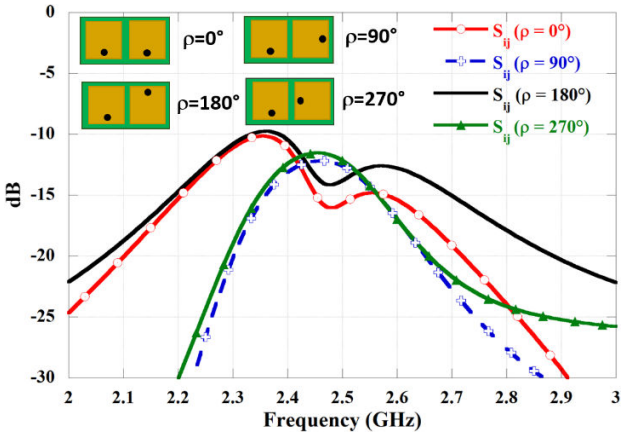

Fig. 10. Mutual coupling as a function of orientation (ρ angle) of the *Element #2* in CP MIMO configuration.

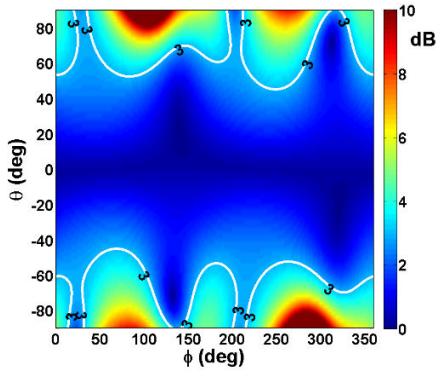

Fig. 11. Simulated *AR* for CP MIMO antenna in the upper hemisphere at 2.45 GHz (Element #1).

(a) *(b)*

Fig. 12. Top view of the fabricated *(a)* CP and *(b)* LP MIMO antenna.

Since the envelope correlation coefficient (ECC) is one of the most important parameter in MIMO antenna configuration, it is necessary to investigate this parameter by using CP and LP radiators. Indeed, the ECC is a measure that describes how much the communication channels are correlated each other [38] and it depends on the antenna radiation pattern (RP) and the environment. Since the antenna considered in the example is designed for indoor WLAN application, an isotropic communication channel has been used for evaluating the correlation [39]. In a uniform propagation environment, the ECC is calculated as [40]:

$$ECC = \frac{\left| \iint_{4\pi} \vec{E}_1(\theta,\phi)\vec{E}_2^*(\theta,\phi)d\Omega \right|^2}{\iint_{4\pi} \left|\vec{E}_1(\theta,\phi)\right|^2 d\Omega \iint_{4\pi} \left|\vec{E}_2(\theta,\phi)\right|^2 d\Omega} \quad (15)$$

where $\vec{E}_l(\theta,\phi) = E_\theta^i \hat{l}_\theta + E_\phi^i \hat{l}_\phi$ is the radiation field of the *l-th* radiating element ($l = 1,2$), and E_θ^i, E_ϕ^i are the field components along θ and ϕ. The measured ECC behaviour with respect to frequency for both CP and LP MIMO antenna configuration is reported in Fig. 13. It proves that within the WLAN band (2.4 GHz – 2.5 GHz) both MIMO configurations present a small ECC for their polarization diversity. However, the employment of the circular polarization allows a lower ECC within the WLAN band.

Moreover, two MIMO antennas with an ECC value comparable to the MIMO state of the art have been employed in order to make a fair comparison.

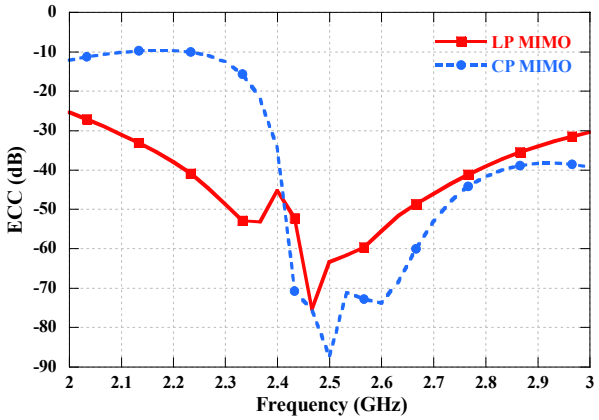

Fig. 13. ECC comparison between CP and LP MIMO antenna.

B. *Received Power (Pr)*

The scenario reported in Fig. 14 has been analysed to evaluate the received power (P_r) for both CP and LP MIMO antenna in an indoor environment. All the items within the room (windows, doors, furniture) have been defined with the appropriate electric properties. More in detail, the transmitter (*Tx*) of the WLAN is placed 3 m above a metallic cabinet whereas twenty receivers (*Rx*) are distributed inside the room (Fig. 14*a*). More in detail, ten MIMO receivers are placed in different positions, five in LOS (red marker) and five in NLOS condition (black marker). Each MIMO antenna (Ant_i) comprises two receivers (Rx_j) where:

$$Ant_i \rightarrow \left(Rx_j, Rx_{j+1}\right) \quad i = 1,\ldots,10;\ j = 2i-1 \quad (16)$$

The P_r by each antenna has been evaluated for both CP and LP radiators by considering the antenna radiation pattern and the propagation inside the indoor environment (Fig. 14*b*).

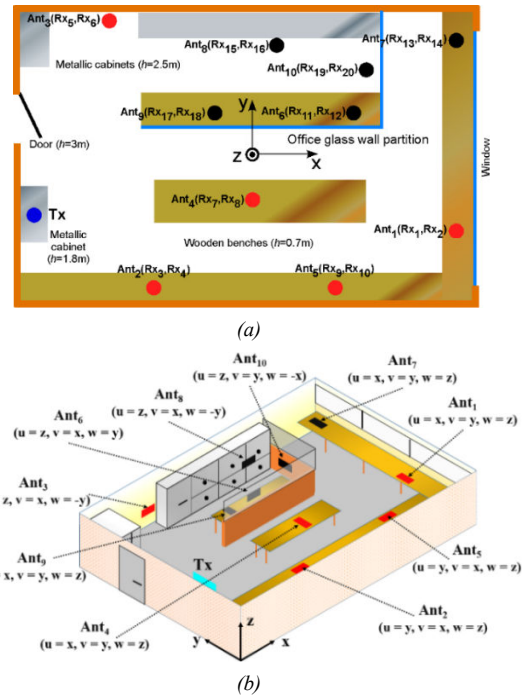

(a)

(b)

Fig. 14. Layout of the simulated indoor scenario: *(a)* top view and *(b)* isometric view with the related radiation pattern direction.

The level of the received power (P_r) for each element of the MIMO antenna, as a function of rotation angle (α), can be seen in Fig. 15 for both CP radiators as well as LP ones. The angle α corresponds to the counterclockwise rotation angle of the MIMO antennas around their normal axis. For example, for Ant_1, the (u,v,w) axis (Fig. 9) will be respectively mapped to the (y, -x, z) axis in correspondence of $\alpha = 90°$. It is apparent that by employing a CP radiators (Fig. 15*a*) the P_r presents lower fluctuations with respect to the antenna orientation (α angle) and a higher average received power both for the LOS and NLOS case. It is therefore clear that the CP MIMO antenna allows achieving a better coverage and reliability of the link of the whole environment.

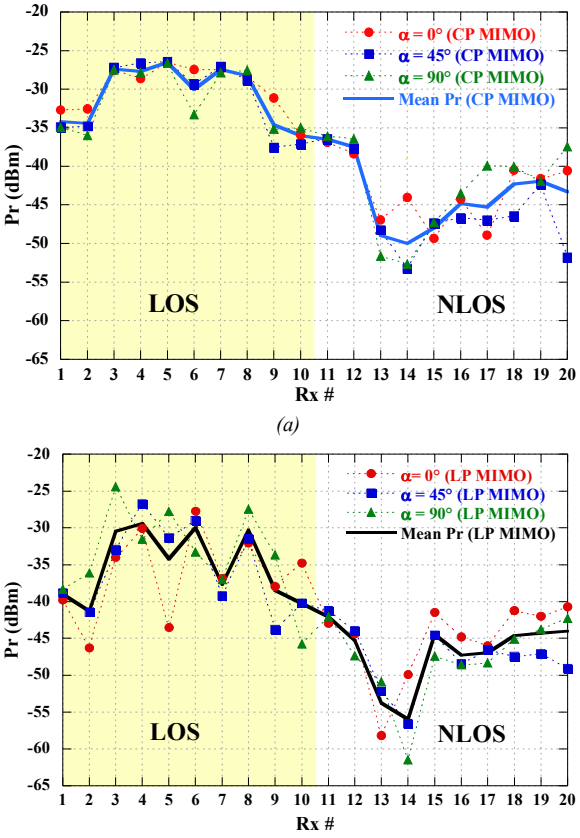

Fig. 15. Received power (P_r) for each element of *(a)* CP and *(b)* LP MIMO antenna as a function of rotation angle (α).

As already mentioned, an important parameter affecting the performance of a MIMO system, in terms of diversity gain (*DG*) and channel capacity (*C*), is the relative power levels of different branches. The branch-power-ratio, defined as the ratio between the minimum power (P_{min}) and maximum power (P_{max}) received by the elements, is shown in Fig. 16. It is evident that CP antenna outperforms the LP antenna in terms of unbalance in power level. Indeed, the 70% of CP MIMO antennas presents a branch-power-ratio greater than -3 dB, and only one with a higher value (*i.e.* – 3.5 dB). On the contrary, the branch-power-ratio of LP MIMO antennas is much more variable and with a minimum value of – 7.34 dB. This unbalance of P_r leads to lower *DG* and *C* of the MIMO system, as it was also evident in the LOS propagation channel matrix ($H_{LOS}^{(LP)}$) previously shown (Fig. 6). Therefore, the benefits of adopting CP radiators in terms of the unbalance P_r is also confirmed in case of multipath propagation condition.

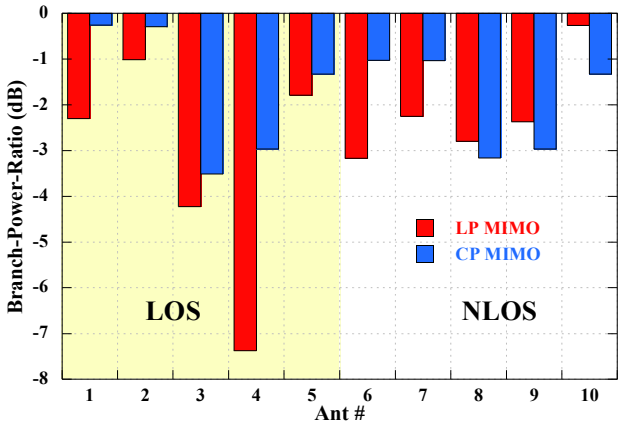

Fig. 16. Branch-Power-ratio in indoor environment by using *(a)* CP and *(b)* LP MIMO antenna system.

IV. Channel Capacity

Channel capacity expresses how many bits can be transmitted by exploiting 1 Hz of bandwidth. When the transmitter is not acquainted of the channel conditions, the power is equally split to each transmitting antenna element and the channel capacity can be expressed as:

$$C = \log_2\left[\det\left(I_{n_R} + \frac{SNR}{n_T} HH^*\right)\right] \tag{17}$$

where I_{nR} is an $n_R \times n_R$ identity matrix, n_R and n_T represent the number of antennas used at receiver and transmitter, respectively, SNR is the signal-to-noise at the receiver and H is the environmental channel matrix. Generally, the entries of H are correlated because of the characteristics of the propagation environment and the antenna elements. In order to calculate the channel matrix H, the Kronecker model [41] has been used due to its simplicity and its ability to consider the effects of antenna correlation, the total efficiency as well as propagation channel. A propagation environment of an independent and identically distributed (i.i.d.) Rayleigh fading channel (H_w) has been assumed to calculate the channel capacity. For this reason, the entries of H_w matrix are i.i.d complex Gaussian values with zero mean and unit variance. The MIMO channel matrix H, adopting the Kronecker model, is given by:

$$H = R_r^{1/2} H_w R_t^{1/2} \tag{18}$$

$$\begin{cases} R_r = \Lambda^{1/2} \overline{R}_r \Lambda^{1/2} \\ R_t = \Lambda^{1/2} \overline{R}_t \Lambda^{1/2} \end{cases} \tag{19}$$

where R_r and R_t are the receiving and transmission matrices, respectively. They account for the coupling among the antennas, calculated with a uniform propagation environment, and the total efficiency as described in [42]. More in detail, $\overline{R}_r$ and $\overline{R}_t$ are a matrix whose diagonal elements are 1, and the off-

diagonal (*i,j*) element denotes the complex correlation coefficient calculated by using the radiation pattern. Λ is a diagonal matrix whose *i-th* element (*i,i*) represents the total efficiency of the *i-th* port (η_{tot}).

The simulated mean channel capacity as a function of the SNR at 2.45 GHz is reported in Fig. 17 for both CP and LP MIMO antenna configuration.

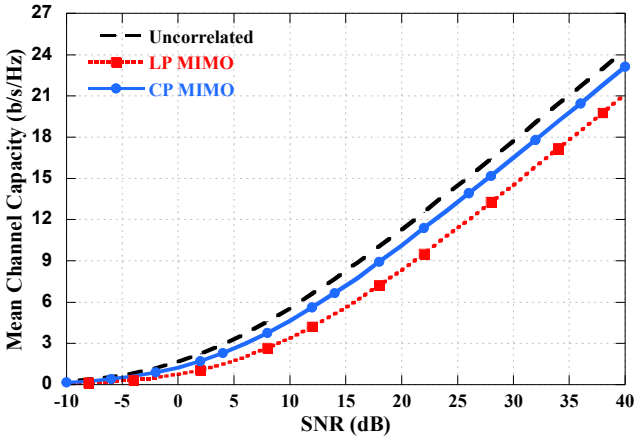

Fig. 17. Comparison among the mean capacity of CP and LP MIMO antenna, as well as an uncorrelated MIMO antenna as a function of SNR by using Kronecker model.

The mean capacity is obtained by averaging 10 000 realization of the propagation channel *H*. For the sake of comparison, it is also reported the average MIMO channel capacity under the assumption of a Rayleigh fading channel and ideal antennas which have zero correlation and 100% total efficiency ($R_r = R_t = I$).

It is evident from Fig. 17 that the mean channel capacity of CP MIMO is higher than LP MIMO configuration, although it is slightly lower than the aforementioned ideal MIMO configuration. Moreover, the mean channel capacity as a function of frequency for a SNR = 30 dB at receiver side is presented in Table III in the case of the WLAN band.

TABLE IIII
MEAN CHANNEL CAPACITY (B/S/HZ) WITH A SNR = 30 DB

Frequency (GHz)	(2x2) Uncorrelated	CP MIMO	LP MIMO
2.4	17.7	16.29	14.53
2.45	17.7	16.51	14.41
2.5	17.7	16.44	14.29

It can be observed that by exploiting the circular polarization and the polarization diversity it is possible to improve the channel capacity. Indeed, CP MIMO outperforms the LP MIMO configuration and it is also very close to the uncorrelated MIMO system with uncorrelated antennas.

In order to further demonstrate the real advantage of using CP antennas in WLAN applications, the mean channel capacity has been also evaluated in an indoor environment.

An Agilent E5071C vector network analyzer has been used to measure the S_{12} parameter necessary to fill the (*i,j*) element of the matrix *H* with the other antennas terminated in 50 Ω loads [6], [33]. In order to remove the effect of path loss, the matrix *H* has been normalized to obtain a unitary average power. This normalization removes the path loss but does not eliminate the effect of antenna correlation and coupling [7]. The channel capacity has been evaluated in both line-of-sight (LOS) end non line-of-sight (NLOS) links. The antennas were placed at a distance of 2 m. To achieve the NLOS condition, a metallic cabinet was placed between the direct path.

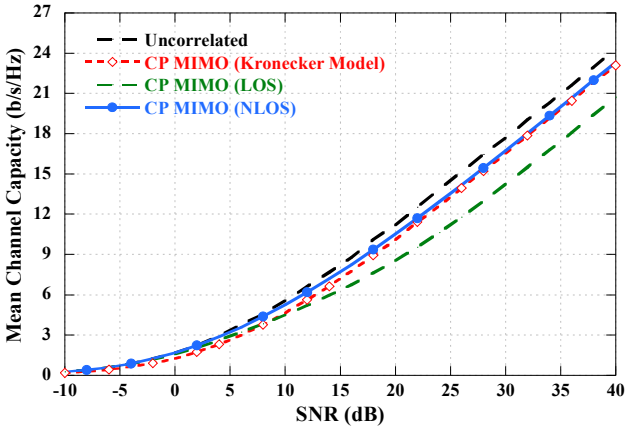

Fig. 18. Measured mean channel capacity of CP MIMO antenna in indoor environment as a function of SNR.

As it is apparent in Fig. 18, the mean channel capacity is greater in NLOS condition because this case represents the most uncorrelated transmission channel. Moreover, the measured mean channel capacity in NLOS scenario confirms the results obtained via the Kronecker model. Indeed, the mean capacity is very close to the Rayleigh fading channel with ideal antennas which have zero correlation and 100% total efficiency ($R_r = R_t = I$). In particular, at SNR = 30 dB the capacity exhibited by CP MIMO was 17.48 b/s/Hz, which is 98.75% of the capacity obtained with ideal uncorrelated antennas. For this reason, CP radiators allows getting performance very close to the ideal case.

V. CONCLUSION

An extensive study on the employment of CP radiators in MIMO system has been proposed in this paper. In particular, the advantages with respect to LP MIMO antennas have been investigated both for the LOS case with only the direct ray as well as for multipath indoor propagation. The channel matrix (H_{LOS}) has been calculated for LOS condition as a function of the antenna parameters and orientation in order to compare the system performance in terms of the eigenvalues and channel capacity. The results of this analysis have proved that CP radiators are capable of obtaining greater eigenvalues, as a function of the MIMO antenna orientation, than LP ones. For this reason, the achievable channel capacity of the CP radiators outperforms the LP ones when the MIMO antennas are not perfectly aligned. Moreover, CP MIMO allows obtaining better performance from a statistical point of view in case which the 3 dB *AR* angle assumes values greater than 40 degrees.

To take into account the effect of multipath propagation, the MIMO system performance in an indoor environment have been evaluated by using a numerical solver as well as with measurements. The level of the received power and the

comparison between the simulated and the measured channel capacity confirm the better performance and reliability of CP antennas with respect to the LP ones. Circularly-polarized antennas can be therefore considered an interesting candidate to be adopted in MIMO systems.

The performance enhancement of MIMO systems employing orthogonally CP radiators has been demonstrated for two orthogonal radiators. For this reason, the capability of orthogonally CP radiators in MIMO antenna with more than two radiators, such as massive MIMO system, needs additional studies and extensive investigations, especially in case of small radiators separation where the correlation between the elements with the same polarization can reach high values and so reduce the overall MIMO performance. A detailed study on this interesting subject is currently ongoing and we plan to provide a detailed analysis, as well as numerical and experimental results in a future work.

VI. Acknowledgments

The authors would like to thank Prof. Buon Kiong Lau for the time he spent with them in stimulating discussions.

References

[1] M. A. Jensen and J. W. Wallace, "A Review of Antennas and Propagation for MIMO Wireless Communications," *IEEE Trans. Antennas Propag.*, vol. 52, no. 11, pp. 2810–2824, Nov. 2004.

[2] Lizhong Zheng and D. N. C. Tse, "Diversity and multiplexing: a fundamental tradeoff in multiple-antenna channels," *IEEE Trans. Inf. Theory*, vol. 49, no. 5, pp. 1073–1096, May 2003.

[3] A. F. Molisch and M. Z. Win, "MIMO systems with antenna selection," *Microw. Mag. IEEE*, vol. 5, no. 1, pp. 46–56, 2004.

[4] J. Valenzuela-valdes, M. Garcia-fernandez, A. Martinez-gonzalez, and D. Sanchez-Hernandez, "The Role of Polarization Diversity for MIMO Systems Under Rayleigh-Fading Environments," *Antennas Wirel. Propag. Lett.*, vol. 5, no. 1, pp. 534–536, Dec. 2006.

[5] M. S. Sharawi, M. U. Khan, A. B. Numan, and D. N. Aloi, "A CSRR Loaded MIMO Antenna System for ISM Band Operation," *IEEE Trans. Antennas Propag.*, vol. 61, no. 8, pp. 4265–4274, Aug. 2013.

[6] W. C. Zheng, L. Zhang, Q. X. Li, and Y. Leng, "Dual-Band Dual-Polarized Compact Bowtie Antenna Array for Anti-Interference MIMO WLAN," *IEEE Trans. Antennas Propag.*, vol. 62, no. 1, pp. 237–246, Jan. 2014.

[7] J. R. Costa, E. B. Lima, C. R. Medeiros, and C. A. Fernandes, "Evaluation of a new wideband slot array for MIMO performance enhancement in indoor WLANs," *Antennas Propag. IEEE Trans. On*, vol. 59, no. 4, pp. 1200–1206, 2011.

[8] R. Karimian, H. Oraizi, S. Fakhte, and M. Farahani, "Novel F-Shaped Quad-Band Printed Slot Antenna for WLAN and WiMAX MIMO Systems," *IEEE Antennas Wirel. Propag. Lett.*, vol. 12, pp. 405–408, 2013.

[9] C.-X. Mao and Q.-X. Chu, "Compact Coradiator UWB-MIMO Antenna With Dual Polarization," *IEEE Trans. Antennas Propag.*, vol. 62, no. 9, pp. 4474–4480, Sep. 2014.

[10] J. Malik, A. Patnaik, and M. Kartikeyan, "Novel Printed MIMO Antenna with Pattern and Polarization Diversity," *IEEE Antennas Wirel. Propag. Lett.*, pp. 1–1, 2014.

[11] Yun-Taek Im, Jee-Hoon Lee, R. A. Bhatti, and Seong-Ook Park, "A Spiral-Dipole Antenna for MIMO Systems," *IEEE Antennas Wirel. Propag. Lett.*, vol. 7, pp. 803–806, 2008.

[12] D. Sievenpiper, L. Zhang, R. F. J. Broas, N. G. Alexopolous, and E. Yablonovitch, "High-impedance electromagnetic surfaces with a forbidden frequency band," *Microw. Theory Tech. IEEE Trans. On*, vol. 47, no. 11, pp. 2059–2074, 1999.

[13] S. Ghosh, T.-N. Tran, and T. Le-Ngoc, "Dual-Layer EBG-Based Miniaturized Multi-Element Antenna for MIMO Systems," *IEEE Trans. Antennas Propag.*, vol. 62, no. 8, pp. 3985–3997, Aug. 2014.

[14] G. Li, H. Zhai, L. Li, C. Liang, R. Yu, and S. Liu, "AMC-Loaded Wideband Base Station Antenna for Indoor Access Point in MIMO System," *IEEE Trans. Antennas Propag.*, vol. 63, no. 2, pp. 525–533, Feb. 2015.

[15] C.-Y. Chiu, C.-H. Cheng, R. D. Murch, and C. R. Rowell, "Reduction of Mutual Coupling Between Closely-Packed Antenna Elements," *IEEE Trans. Antennas Propag.*, vol. 55, no. 6, pp. 1732–1738, Jun. 2007.

[16] H. Arun, A. K. Sarma, M. Kanagasabai, S. Velan, C. Raviteja, and M. G. N. Alsath, "Deployment of Modified Serpentine Structure for Mutual Coupling Reduction in MIMO Antennas," *IEEE Antennas Wirel. Propag. Lett.*, vol. 13, pp. 277–280, 2014.

[17] S. Zhang, B. K. Lau, Y. Tan, Z. Ying, and S. He, "Mutual Coupling Reduction of Two PIFAs With a T-Shape Slot Impedance Transformer for MIMO Mobile Terminals," *IEEE Trans. Antennas Propag.*, vol. 60, no. 3, pp. 1521–1531, Mar. 2012.

[18] H. Li, B. K. Lau, Z. Ying, and S. He, "Decoupling of Multiple Antennas in Terminals With Chassis Excitation Using Polarization Diversity, Angle Diversity and Current Control," *IEEE Trans. Antennas Propag.*, vol. 60, no. 12, pp. 5947–5957, Dec. 2012.

[19] S. Zhang, B. K. Lau, A. Sunesson, and S. He, "Closely-Packed UWB MIMO/Diversity Antenna With Different Patterns and Polarizations for USB Dongle Applications," *IEEE Trans. Antennas Propag.*, vol. 60, no. 9, pp. 4372–4380, Sep. 2012.

[20] J. Zhu, S. Li, B. Feng, L. Deng, and S. Yin, "Compact Dual-Polarized UWB Quasi-Self-Complementary MIMO/Diversity Antenna With Band-Rejection Capability," *IEEE Antennas Wirel. Propag. Lett.*, vol. 15, pp. 905–908, 2016.

[21] W. Lin and H. Wong, "Wideband Circular Polarization Reconfigurable Antenna," *IEEE Trans. Antennas Propag.*, vol. 63, no. 12, pp. 5938–5944, Dec. 2015.

[22] S. Gao, Q. Luo, and F. Zhu, *Circularly polarized antennas*. Chichester, West Sussex, United Kingdom: John Wiley & Sons Inc, 2014.

[23] Yuan Yao, Xing Wang, Xiaodong Chen, Junsheng Yu, and Shaohua Liu, "Novel Diversity/MIMO PIFA Antenna With Broadband Circular Polarization for Multimode Satellite Navigation," *IEEE Antennas Wirel. Propag. Lett.*, vol. 11, pp. 65–68, 2012.

[24] Jung-Hoon Han and Noh-Hoon Myung, "Novel Feed Network for Circular Polarization Antenna Diversity," *IEEE Antennas Wirel. Propag. Lett.*, vol. 13, pp. 979–982, 2014.

[25] J. Wang, Z. Lv, and X. Li, "Analysis of MIMO Diversity Improvement Using Circular Polarized Antenna," *Int. J. Antennas Propag.*, vol. 2014, pp. 1–9, 2014.

[26] M. Coldrey, "Modeling and capacity of polarized MIMO channels," in *Vehicular Technology Conference, 2008. VTC Spring 2008. IEEE*, 2008, pp. 440–444.

[27] G. Tiberi, S. Bertini, W. Q. Malik, A. Monorchio, D. J. Edwards, and G. Manara, "Analysis of Realistic Ultrawideband Indoor Communication Channels by Using an Efficient Ray-Tracing Based Method," *IEEE Trans. Antennas Propag.*, vol. 57, no. 3, pp. 777–785, Mar. 2009.

[28] R. Mittra, Ed., *Computational Electromagnetics*. New York, NY: Springer New York, 2014.

[29] J. F. Valenzuela-Valdes, M. A. Garcia-Fernandez, A. M. Martinez-Gonzalez, and D. A. Sanchez-Hernandez, "Evaluation of True Polarization Diversity for MIMO Systems," *IEEE Trans. Antennas Propag.*, vol. 57, no. 9, pp. 2746–2755, Sep. 2009.

[30] W.-J. Liao, S.-H. Chang, J.-T. Yeh, and B.-R. Hsiao, "Compact dual-band WLAN diversity antennas on USB dongle platform," *Antennas Propag. IEEE Trans. On*, vol. 62, no. 1, pp. 109–118, 2014.

[31] Y. Gao, X. Chen, Z. Ying, and C. Parini, "Design and Performance Investigation of a Dual-Element PIFA Array at 2.5 GHz for MIMO Terminal," *IEEE Trans. Antennas Propag.*, vol. 55, no. 12, pp. 3433–3441, Dec. 2007.

[32] J. O. Nielsen, B. Yanakiev, S. Caporal Del Barrio, and G. F. Pedersen, "On Antenna Design Objectives and the Channel Capacity of MIMO Handsets," *IEEE Trans. Antennas Propag.*, vol. 62, no. 6, pp. 3232–3241, Jun. 2014.

[33] G. V. Tsoulos, Ed., *MIMO system technology for wireless communications*. Boca Raton [Fla.]: CRC/Taylor & Francis, 2006.

[34] J. P. Kermoal, L. Schumacher, K. I. Pedersen, P. E. Mogensen, and F. Frederiksen, "A stochastic MIMO radio channel model with experimental validation," *IEEE J. Sel. Areas Commun.*, vol. 20, no. 6, pp. 1211–1226, Aug. 2002.

[35] T. Yoo and A. Goldsmith, "Capacity and power allocation for fading MIMO channels with channel estimation error," *IEEE Trans. Inf. Theory*, vol. 52, no. 5, pp. 2203–2214, 2006.

[36] F. Rusek, D. Persson, Buon Kiong Lau, E. G. Larsson, T. L. Marzetta, and F. Tufvesson, "Scaling Up MIMO: Opportunities and Challenges

with Very Large Arrays," *IEEE Signal Process. Mag.*, vol. 30, no. 1, pp. 40–60, Jan. 2013.

[37] Ka Yan Lam, Kwai-Man Luk, Kai Fong Lee, Hang Wong, and Kung Bo Ng, "Small Circularly Polarized U-Slot Wideband Patch Antenna," *IEEE Antennas Wirel. Propag. Lett.*, vol. 10, pp. 87–90, 2011.

[38] M. S. Sharawi, "Printed Multi-Band MIMO Antenna Systems and Their Performance Metrics [Wireless Corner]," *Antennas Propag. Mag. IEEE*, vol. 55, no. 5, pp. 218–232, 2013.

[39] M. P. Karaboikis, V. C. Papamichael, G. F. Tsachtsiris, C. F. Soras, and V. T. Makios, "Integrating Compact Printed Antennas Onto Small Diversity/MIMO Terminals," *IEEE Trans. Antennas Propag.*, vol. 56, no. 7, pp. 2067–2078, Jul. 2008.

[40] S. Blanch, J. Romeu, and I. Corbella, "Exact representation of antenna system diversity performance from input parameter description," *Electron. Lett.*, vol. 39, no. 9, pp. 705–707, May 2003.

[41] Liang Dong, Hosung Choo, R. W. Heath, and Hao Ling, "Simulation of MIMO channel capacity with antenna polarization diversity," *IEEE Trans. Wirel. Commun.*, vol. 4, no. 4, pp. 1869–1873, Jul. 2005.

[42] Ruiyuan Tian, Buon Kiong Lau, and Zhinong Ying, "Multiplexing Efficiency of MIMO Antennas," *IEEE Antennas Wirel. Propag. Lett.*, vol. 10, pp. 183–186, 2011.

[43] H. Nishimoto, Y. Ogawa, T. Nishimura, and T. Ohgane, "Measurement-Based Performance Evaluation of MIMO Spatial Multiplexing in a Multipath-Rich Indoor Environment," *IEEE Trans. Antennas Propag.*, vol. 55, no. 12, pp. 3677–3689, Dec. 2007.